

Design, Synthesis and Biological Evaluation of Nitro Oxide Donating *N*-Hydroxycinnamamide Derivatives as Histone Deacetylase Inhibitors

Shiliang Tu,*^a Hang Yuan,^a Jie Hu,^b Chengguang Zhao,^b Rui Chai,^a and Hongfeng Cao^a

^aDepartment of Coloproctology, Zhejiang Provincial People's Hospital; Hangzhou 310014, P.R. China; and

^bDepartment of Pharmacy, Wenzhou Medical University; Wenzhou 325000, P.R. China.

Received June 17, 2014; accepted September 19, 2014

Novel nitro oxide (NO)-donating *N*-hydroxycinnamamide derivatives 12a–j were designed and synthesized by coupling the carboxyl group of *N*-hydroxycinnamamides with phenylsulfonylfuroxan through various diols or alkylol amines, and their *in vitro* biological activities were evaluated. It was discovered that most of target compounds showed good histone deacetylases (HDACs) inhibition and anti-tumor activities, particularly for 12j, which had great HDACs inhibitory activities (IC_{50} s=0.15–0.26 μ M) and antiproliferative effects (IC_{50} s=3.21–7.12 μ M) comparable to suberoylanilide hydroxamic acid (SAHA) (IC_{50} s=0.16–1.41 μ M for HDACs, IC_{50} s=3.15–7.45 μ M for cancer cell inhibition). Furthermore, compound 12j with strong antitumor activities produced high levels of NO (up to 8.0 μ M of nitrites/nitrates) in colon cancer cells, and its antiproliferative activity was nearly half-diminished by hemoglobin (10 μ M), an NO scavenger. These results suggest that the strong antiproliferative activity of 12j could be attributed to the additive effects of high levels of NO production and inhibition of HDAC in the cancer cells.

Key words nitro oxide; histone deacetylase inhibitor; furoxan; *N*-hydroxycinnamamide; anti-tumor agent

Pharmacological targeting of proteins that regulate epigenetics has emerged as a promising therapeutic area of study.^{1,2} Epigenetic or chromatin modification is recognized by nonhistone proteins and is a code of gene expression. Among the various histone modifiers, Histone acetyltransferase (HAT) and histone deacetylase (HDAC) are two reversible enzymes regulating histone acetylation status and executing the acetylation and deacetylation of the lysine residues at the amino terminal of histones.³ However, abnormal HDAC overexpression has been found to be involved in the development of several kinds of human cancers, including myeloid neoplasia and solid tumors.⁴ Recent studies have shown that acetylation of non-histone proteins is also relevant for tumorigenesis, cancer cell proliferation, and immune functions.⁵ Consequently, histone deacetylases are considered to be important targets in the development of anticancer agents, and in recent years considerable attention has been paid to HDAC inhibitors (HDACI) as anticancer agents.^{6–8}

There has been a high level of interest in developing small-molecule HDACI, and numerous structurally diverse HDACI have been developed as potential anticancer agents, which are grouped chemically into four classes: hydroxamic acids, benzamides, cyclic tetrapeptides, and short-chain fatty acids.⁹ The common pharmacophore of these HDACI consists of three domains: a zinc-binding group (ZBG), such as hydroxamic acid; a cap group, generally a hydrophobic and aromatic group; a saturated or unsaturated linker domain, composed of linear or cyclic structures that connect the ZBG and the cap group. Up to now, two of these HDACI, suberoylanilide hydroxamic acid (SAHA, Fig. 1) and cyclic peptide Romidepsin (FK228), have been approved by the U.S. Food and Drug Administration (FDA) for the treatment of cutaneous T-cell lymphoma (CTCL), validating HDACs' potential as an important target for anticancer therapy.^{10,11} Other compounds in clinical trials include hydroxamic acids such as belinostat (PXD101), panobinostat (LBH589), and pracinostat (SB-939) with an *N*-hy-

droxyacrylamide moiety exhibiting excellent HDAC inhibitory activity,^{12–14} benzamides^{15,16} such as entinostat (MS-275), mocetinostat (MGCD-0103), and aliphatic acids, such as valproic acid.¹⁷ In addition, the selective isotype HDAC6 inhibitor, ACY-1215, is currently undergoing human clinical trials for the treatment of multiple myeloma.¹⁸ Among these approved or clinical HDACI, PXD101, LBH589, and SB-939 share a common active fragment, *N*-hydroxycinnamamide. This fragment could not only form bichelation with the active site Zn²⁺ by its hydroxamic acid group but also form a sandwichlike π – π interaction by inserting its vinyl benzene group into two parallel phenylalanine residues of HDAC.^{19,20}

Nitro oxide (NO), which is naturally generated from L-arginine by the action of NO synthase (NOS), is a key signaling and effector molecule and plays a pivotal role in diverse physiological and pathophysiological processes.²¹ It is well-known that high concentration of NO, generated from synthetic NO-releasing compounds, could not only have strong cytotoxicity against human carcinoma cells and induce the apoptotic of tumor cells, but also prevent tumors from metastasizing and sensitize tumor cells to chemotherapy, radiation and immunotherapy *in vitro* and *in vivo*.²² As an important class of NO donors, furoxans such as phenylsulfonylfuroxans are thermally stable compounds and can produce high levels of NO *in vitro* and inhibit the growth of tumors *in vivo*.²³ Furthermore, it was reported that tumor cells are more sensitive to relative high concentration of NO than normal cells and a variety of phenylsulfonylfuroxan-based NO releasing compounds have been investigated to show selective antitumor activity *in vitro* and *in vivo*.^{23–27}

It is known that the Class I enzyme HDAC2 can be directly or indirectly modified by NO, undergoing either Tyr-nitration or *S*-nitrosylation.²⁸ One example of NO-donor HDACI, which is able to simultaneously release NO and regulate HDACs, affects a number of micro-RNAs and synergistically promotes myogenic differentiation.²⁹ It is therefore of high interest to investigate whether introduction of phenylsulfonylfuroxan moiety to the *N*-hydroxycinnamamides would provide

The authors declare no conflict of interest.

* To whom correspondence should be addressed. e-mail: shiliang_tu@126.com

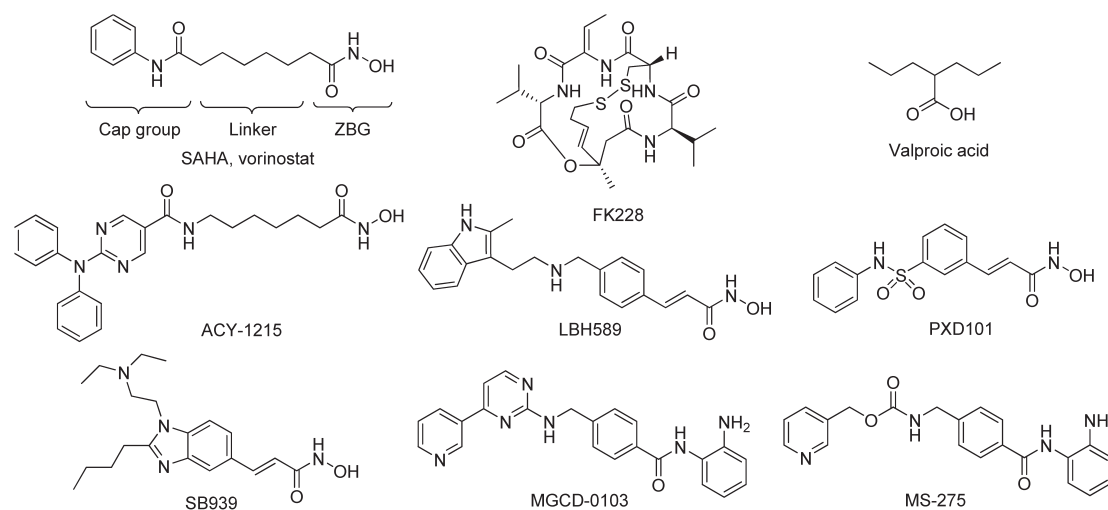
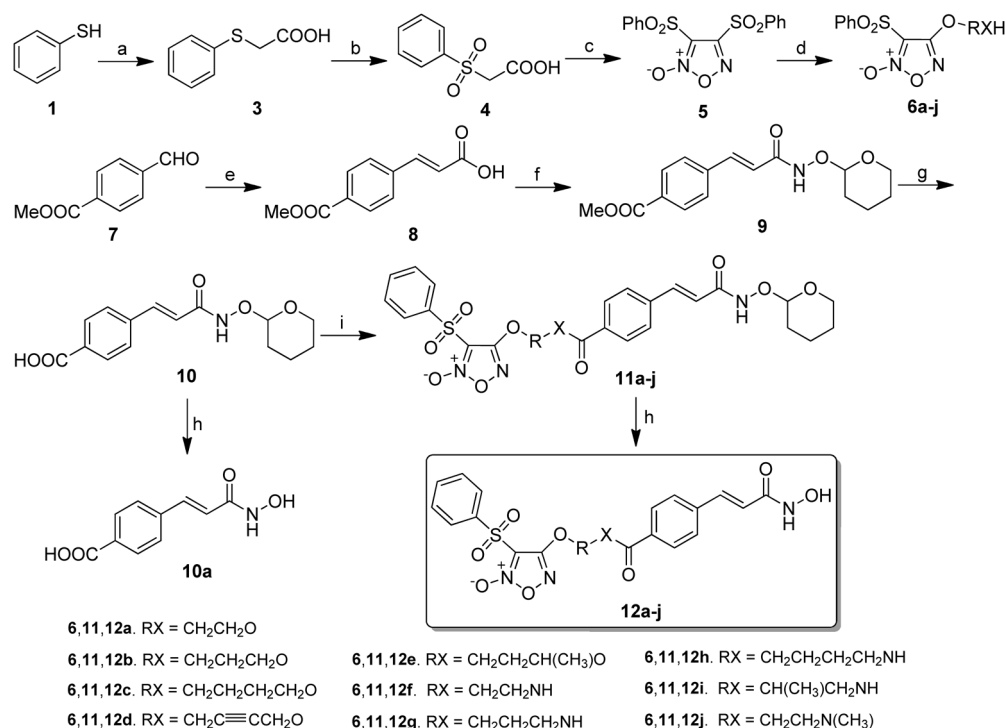


Fig. 1. Structures of Representative HDAC Inhibitors



Reagents and conditions: a) 1. NaOH (aq.), 140°C, 2h; 2. conc. HCl; (b) 30% H₂O₂, AcOH, rt, 3h; (c) fuming nitric acid, 90°C, 4h; (d) diols or alkylol amines, THF, 30% NaOH, rt, 4–8h; (e) propanedioic acid, piperidine, pyridine, 85°C, 3h; (f) 1. ethyl chloroformate, *N*-methylmorpholine, THF, 0°C to rt, 1h; 2. tetrahydro-2*H*-pyran-2-ol, TEA, THF, 0°C, 1h; (g) 1M NaOH (aq.), MeOH, rt, 2h; (h) TFA, CH₂Cl₂, rt, 2–4h; (i) 6a–j, EDCI, DMAP, CH₂Cl₂, rt, 10–15h.

Chart 1

a hitherto unknown class of NO donating HDAC inhibitors that may effectively develop inhibitory effect of HDACs and release high levels of NO with an additive effect for treatment of cancer. As part of our ongoing research program, a series of phenylsulfonylfuroxan-based *N*-hydroxycinnamide derivatives **12a–j** were designed and synthesized by coupling the carboxyl of *N*-hydroxycinnamides with phenylsulfonylfuroxan through different carbochain length substituted diols or alkylol amines.

Chemistry

The synthesis of **12a–j** was described in Chart 1. The substituted furoxans **6a–j** were prepared in a four step se-

quence. Thiophenol **1** as the starting material was converted to 2-(phenylthio)acetic acid **3** by treatment with chloroacetic acid **2** in 97% yield. Oxidation of **3** using 30% H₂O₂ aqueous solution in acetic acid afforded 2-(phenylsulfonyl)acetic acid **4**, which was directly reacted with fuming nitric acid to form diphenylsulfonylfuroxan **5**. Compound **5** was then converted to various monophenylsulfonylfuroxans **6a–j** by treatment with corresponding diol or alkylol amines. On the other hand, methyl 4-formylbenzoate **7** was reacted with propanedioic acid in the presence of piperidine to give (*E*)-3-(4-(methoxycarbonyl)phenyl)acrylic acid **8**, which was further treated with tetrahydro-2*H*-pyran-2-ol to form compound **9** in the presence of *N*-methylmorpholine and ethyl chloroformate.

Table 1. Inhibition of HeLa Nuclear HDACs by **12a–j**

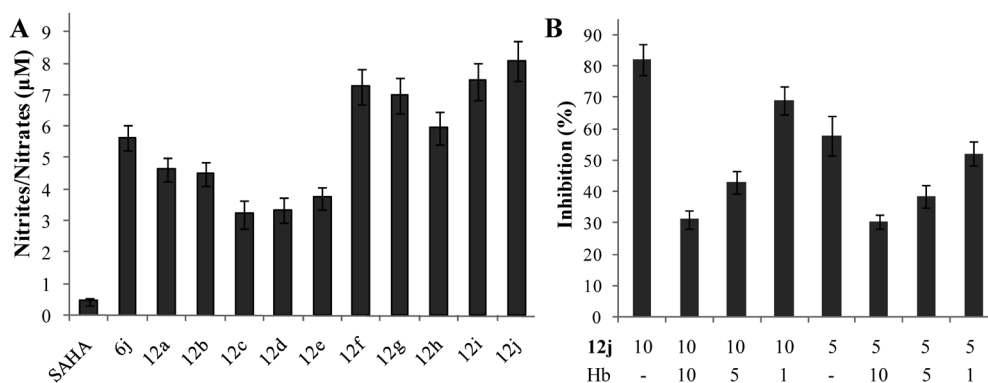
Compd.	IC ₅₀ ^{a)} (μM)	Compd.	IC ₅₀ ^{a)} (μM)
SAHA	0.17	12f	0.18
12a	0.55	12g	0.21
12b	0.86	12h	0.59
12c	>1	12i	0.25
12d	>1	12j	0.15
12e	>1		

^{a)} The data are the mean values of IC₅₀ from at least three independent experiments.

Table 2. IC₅₀ Value for the Inhibition of HDACs 2, 6, and 8 by **12f, g** and **12i, j**

Compd.	IC ₅₀ ^{a)} (μM)		
	HDAC2	HDAC6	HDAC8
SAHA	0.18	0.16	1.41
6j	0.43	ND ^{b)}	ND
12f	0.16	0.15	0.29
12g	ND	0.23	0.46
12i	ND	0.28	0.42
12j	ND	0.16	0.26

^{a)} The data are the mean values of IC₅₀ from at least three independent experiments. ^{b)} Not detected.

Fig. 2. NO Release Behaviors of the Indicated Compounds and Their Correlation with *in Vitro* Antiproliferative Activities

(A) Quantitative measurement of intracellular NO production. HCT116 cells were treated with various compounds (50 μM) for 6 h, and the amounts of intracellular nitrite/nitrate were determined using a colorimetric Griess reaction assay. Data are expressed as means ± S.D. from three separate experiments. (B) HCT116 cells were pre-treated with, or without, the indicated concentrations of NO scavenger hemoglobin (Hb) for 1 h and treated with 5 or 10 μM of **12j** for 24 h. The cell growth was determined by the MTT. Data are expressed as mean% of inhibition on the growth of HCT116 cells from three independent experiments. The cells treated with different concentrations of hemoglobin alone did not affect their growth (data not shown).

Compound **9** was subsequently hydrolyzed to obtain intermediate **10**, which were directly treated with **6a–j** in CH₂Cl₂ in the presence of 1-(3-dimethyl aminopropyl)-3-ethylcarbodi-imide hydrochloride (EDCI) and 4-dimethylamino pyridine (DMAP) to generate **11a–j**, respectively. Finally, *O*-protected groups of **10** and **11a–j** were removed by CF₃COOH to provide **10a** and **12a–j**. The products **12a–j** were purified by column chromatography, and their structures were characterized by IR, ¹H-NMR, MS, and elemental analyses.

Results and Discussion

All synthesized compounds **12a–j** were evaluated for their ability to inhibit HeLa cell nuclear HDACs (which consist of mostly HDAC1–3), with SAHA as a reference compound. The values of half inhibitory concentration (IC₅₀) about all the target compounds against HeLa cell nuclear HDACs were measured and presented in Table 1. The results indicated the HDACs inhibitory activities of ester derivatives **12a–e** were slightly weaker than those of amide compounds **12f–j**, which suggested the amide bond of **12f–j** could be beneficial for them to bind to the active site. Moreover, among these amide compounds, compound **12j** possessed the strongest HeLa nuclear HDACs inhibition comparable to that of SAHA.

Furthermore, the active compounds **12f** and **g**, **12i** and **j**, and NO donor moiety **6j** (the intermediate of **12j**) was further tested for their *in vitro* HDACs inhibitory activities toward HDAC2, HDAC6 and HDAC8 in order to know whether active compounds possessed strong HDACs inhibitory effects

and isoform selectivity. Results listed in Table 2 showed that **12f** and **g** and **12i** and **j** exhibited significant HDACs inhibitory activities against HDACs 2, 6, and 8. Both **12j** and NO donor moiety **6j** demonstrated significant effects on HDAC2 comparable to SAHA, which may partially be due to NO release from **12j** or **6j** inducing *S*-nitrosylation of HDAC2.^{29,30} Furthermore, compounds **12f** and **g** and **12i** and **j** also showed stronger inhibitory potency than SAHA for HDAC8. However, the active compounds **12f** and **g** and **12i** and **j** did not exhibit any isoform selectivity in the HDACs inhibitory assay.

Next, we tested whether the levels of NO production upon treating HCT116 cells with target compounds were associated with their antitumor activities. The levels of nitrite/nitrate produced in the cell lysates of different types of cells were characterized using the Griess assay. As can be seen in Fig. 2A, treatment with SAHA resulted in little nitrite/nitrate. In contrast, treatment with **12f–j** produced high levels of nitrite/nitrate in HCT116 cells. The most potent compound **12j** released the highest levels of NO, and the derivatives with lower antiproliferative activity released less NO under the same conditions. These results indicate that the amounts of intracellular NO release were well associated with their *in vitro* antiproliferative activity. To further determine the contribution of NO to the inhibitory activities of NO-donating *N*-hydroxycinnamide derivatives, **12j** was selected for testing its antiproliferative activity in the presence or absence of NO scavenger hemoglobin (Hb). HCT116 cells were pre-treated with, or without, different concentrations of Hb for 1 h and then

treated with the indicated concentrations of **12j**. The effects of different treatments on the growth of HCT116 cells were determined by the 3-(4,5-dimethylthiazol-2-yl)-2,5-diphenyltetrazolium bromide (MTT) assays (Fig. 2B). Treatment with **12j** alone greatly inhibited the growth of HCT116 cells, while the inhibitory effects of **12j** on the growth of HCT116 cells were dramatically reduced by pre-treatment with Hb, which appeared to be dose-dependent. Similar patterns of reduced levels of nitrate/nitrite in the cell lysates were observed. These data clearly demonstrated that high levels of NO production by the compound contributed to its antiproliferative activity against human cancer cells *in vitro*.

Next, synthetic compounds **11j**, **12a–j** were also assessed for anti-proliferative activities against five human cancer cells HCT116, SW620, Lovo (human colon carcinoma cells), MCF-7 (human breast adenocarcinoma cells), and Hela were evaluated by MTT assays *in vitro*, with SAHA as positive control. The values of half inhibitory concentration (IC_{50}) about all the target compounds against each tumor cell line were measured and presented in Table 3. For most of the compounds tested, the cell growth inhibition results were consistent with the HDAC inhibition profiles. Most of the target compounds displayed good to moderate antiproliferative activities. The antitumor activities of ester derivatives **12a–e** were slightly weaker than those of amide compounds **12f–j**. What's more, compound **12j** exhibited strongest antiproliferative activities with IC_{50} values of 3.21–7.12 μM against each tested cancer cell, which were comparable to SAHA (IC_{50} s=3.15–7.45 μM). Interestingly, compound **11j** (the intermediate of **12j**, IC_{50} s=9.12–11.4 μM) displayed weak cancer inhibitory activities, which were 2–3-fold less than those of **12j**. Such phenomenon suggested that the hydroxamic acid moiety has a positive influence on the cytotoxicity of this series of *N*-hydroxyferulicamide derivatives.

As active compound **12j** consists of NO donor moiety (**6j**) and the *N*-hydroxycinnamamide moiety (**10a**) (Chart 1), the inhibitory effects of these two moieties on HCT116 cells were examined at two different concentrations. As shown in Fig. 3, the NO-donating moiety **6j** retained a certain degree of inhibitory potency, which was similar to the *N*-hydroxycinnamamide moiety **10a**. And both of them were obviously less potent than **12j**. However, the combination of **10a** with **6j** significantly

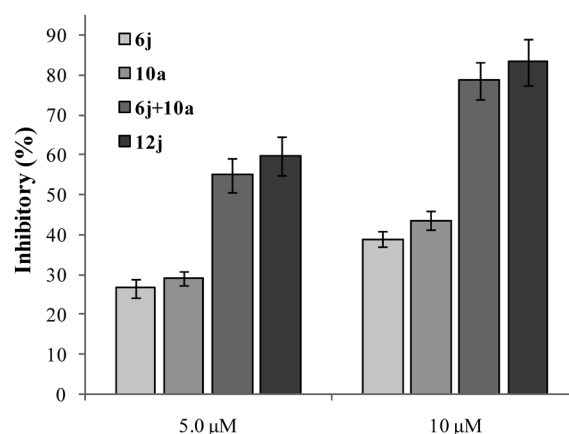


Fig. 3. Inhibitory Activity of **6j**, **10a**, **11j**, and **12j** against HCT116 Cells

HCT116 cells were incubated with the indicated compounds at 5.0 and 10 μM for 24h, and cell proliferation was assessed by the MTT assay. Data are means \pm S.D. of the inhibition (%) from three independent experiments.

induced tumor cell antiproliferative effect comparable to **12j**. These results suggest that the antitumor activity of **12j** may be attributed to the additive effects of phenylsulfonylfuroxan and the *N*-hydroxycinnamamide moiety and that both of them may play crucial roles in the antiproliferative activity of **12j**.

Structure–Activity Relationship (SAR) Analysis of SAR revealed that **12a–j** with different linkers displayed variable antitumor activities. The compounds **12f–j** linked with alkanolamine exhibited stronger inhibitory effects than the ester derivatives **12a–e** linked with diol against human cancer cells. It is likely that the ester compounds can usually be metabolized into the corresponding acid and alcohol, which may lead to the partial loss of their inhibitory activity. In addition, variations in the carbochain lengths of linkers significantly affected the *in vitro* anticancer activity of these derivatives. For example, the compounds **12a**, **12f** and **12j** with a two-carbon diol or alkylol amine showed relatively stronger anticancer activity than compounds with a three- or four-carbon linker. However, further investigation about the precise SAR of these compounds is ongoing.

Conclusion

In summary, a series of novel NO-donating HDAC in-

Table 3. The IC_{50} Values of **11j** and **12a–j** against Five Human Cancer Cell Lines

Compd.	<i>In vitro</i> inhibition of human cancer cells proliferation (IC_{50}^a , μM)				
	Hela	HCT116	SW620	Lovo	MCF-7
SAHA	3.15	5.83	4.72	5.56	7.45
11j	12.5	9.69	11.3	12.6	14.1
12a	9.51	9.47	9.12	10.5	11.4
12b	15.2	14.7	13.9	16.8	18.3
12c	25.8	21.6	20.5	24.6	27.5
12d	21.0	17.9	19.2	19.4	22.7
12e	15.8	13.6	15.0	18.6	16.4
12f	5.02	4.67	5.53	6.65	6.28
12g	6.71	5.78	6.14	8.17	7.18
12h	13.9	12.7	11.9	14.5	15.0
12i	7.27	6.89	7.46	8.75	9.59
12j	4.18	3.21	4.43	5.03	7.12

^a) The inhibitory effects of individual compounds on the proliferation of cancer cell lines were determined by the MTT assay. The data are the mean values of IC_{50} from at least three independent experiments.

hibitors **12a–j** were designed and synthesized by coupling the carboxyl group of *N*-hydroxycinnamamide with phenylsulfonylfuroxan through various carbochain length substituted diols or alkylol amines. The *in vitro* assay of their inhibitory activities against five human cancer cell lines showed that the phenylsulfonyl-furoxan-based *N*-hydroxycinnamamide derivatives displayed good to moderate antiproliferative activities. Especially, compound **12j** had greater antiproliferation and HDACs inhibitory activities, comparable to SAHA, in human carcinoma cells. What's important, the compounds with strong antitumor activities against human cancer cells produced high levels of NO in colon cancer cells. In addition, the inhibitory effects of **12j** were diminished by NO scavenger Hb in a dose-dependent manner, suggesting that NO released by this compound may play an important role in antiproliferation of HCT116 cells. Our findings suggest that the NO-donating HDAC inhibitors may hold greater promise as therapeutic agents for the intervention of human cancers.

Experimental

Melting points of individual compounds were determined on a Mel-TEMP II melting point apparatus and uncorrected. Infrared (IR) spectra (KBr) were recorded on a Nicolet Impact 410 instrument (KBr pellet). ¹H-NMR was recorded with a Bruker Avance 300MHz spectrometer at 303 K, with chemical shift in parts per million (ppm, δ) downfield from tetramethylsilane, or trimethylsilyl (TMS) as an internal standard. MS spectra were recorded on a Mariner Mass Spectrum (electrospray ionization (ESI)) and HR-MS on Agilent technologies LC/MSD time-of-flight (TOF). Element analysis was performed on an Eager 300 instrument. All compounds were routinely checked by TLC and ¹H-NMR. TLCs and preparative thin-layer chromatography were performed on silica gel GF/UV 254, and the chromatograms were conducted on silica gel (200–300 mesh, Merck) and visualized under UV light at 254 and 365 nm. Thiophenol **1** and compounds **7** were commercially available, and compounds **3–5** and **6a–j** were prepared according the literatures.^{24–26} All solvents were reagent grade and, when necessary, were purified and dried by standards methods. Solutions after reactions and extractions were concentrated using a rotary evaporator operating at a reduced pressure of *ca.* 20 Torr. Organic solutions were dried over anhydrous sodium sulfate.

(E)-3-(4-(Methoxycarbonyl)phenyl)acrylic Acid 8 To a flask was added methyl 4-formylbenzoate **7** (1.64 g, 10 mmol), propanedioic acid (1.56 g, 15 mmol), piperidine (0.08 mL, 0.81 mmol), and pyridine (10 mL) at room temperature. The reaction mixture was heated to 85°C for 3 h under a steady flow of nitrogen gas, cooled to room temperature, and poured into 2 M aqueous HCl (100 mL). The resulting mixture was cooled to 0°C and filtered. The filter cake washed with acetonitrile (2 × 10 mL), and dried *in vacuo* to afford **8** as white solid, yield 85%, mp: 140–142°C.

(E)-4-(3-Oxo-3-(((tetrahydro-2H-pyran-2-yl)oxy)amino)prop-1-en-1-yl)benzoic Acid 10 To a solution of **8** (1.65 g, 8 mmol) in 50 mL anhydrous tetrahydrofuran (THF) at 0°C were added *N*-methylmorpholine (1.05 g, 12 mmol) and ethyl carbonochloridate (0.87 g, 8 mmol), and the mixture was stirred at room temperature for 1 h, which was then added dropwise to a solution of tetrahydro-2H-pyran-2-ol (0.94 g, 8 mmol) in 10 mL anhydrous THF. After the reaction was

completed, the resulting mixture was allowed to pour into ice-water, and extracted with ethyl acetate (30 mL × 3). The organic phase was washed with water and brine, then dried over anhydrous sodium sulfate, filtered and evaporated to afford the crude product, which was poured into 5 mL methanol containing 1.5 mL 2 N NaOH and continuously stirred for 2 h. After the mixture being cooled, the solvent was evaporated, and the residue was neutralized to pH=3 with 1 M HCl. The precipitate was filtered, washed with water, and dried *in vacuo* to afford the crude, which was purified by column chromatography on silica gel to give compound **10** as pale yellow waxy solid, yield 56%, MS (ESI) m/z =292 [M+H]⁺.

(E)-4-(3-(Hydroxyamino)-3-oxoprop-1-en-1-yl)benzoic Acid (10a) A solution of **10** (0.23 g, 0.80 mmol) and CF₃COOH (1 mL) in 4 mL dry CH₂Cl₂ was stirred at room temperature for 2 h. The solvent was removed under reduced pressure. The crude residue was dissolved in 15 mL dichloromethane and 2 mL Et₃N was slowly added to the solvent, and the crude product was purified by column chromatography (MeOH–CH₂Cl₂=1:6–1:10) to yield **10a** as white waxy solid, yield 88%. Analytical data for **10a**: MS (ESI) m/z =208 [M+H]⁺; ¹H-NMR (DMSO-*d*₆, 300 MHz, δ ppm): 10.33 (br, 1H), 8.57 (br, 1H), 7.86 (d, J =7.8 Hz, 2H, Ar-H), 7.66 (d, J =7.8 Hz, 2H, Ar-H), 7.50 (d, J =16.2 Hz, 1H, CH=), 6.55 (d, J =16.2 Hz, 1H, CH=).

General Procedure for the Synthesis of 12a–j Compound **10** (0.23 g, 0.80 mmol) was mixed with **6a–j** (0.80 mmol), EDCI (153 mg, 0.8 mmol), DMAP (97 mg, 0.80 mmol). The mixture was stirred at room temperature for 8–12 h. After filtration, the filtrate was evaporated to dryness *in vacuo*, and poured into 4 mL dry CH₂Cl₂ containing 1 mL CF₃COOH in was stirred at room temperature for 1–2 h. The solvent was removed under reduced pressure. The crude residue was dissolved in 15 mL dichloromethane and 2 mL Et₃N was slowly added to the solvent, and the crude product was purified by column chromatography (MeOH–CH₂Cl₂=1:6–1:10) to yield **12**.

(E)-4-(2-(((4-(3-(Hydroxyamino)-3-oxoprop-1-en-1-yl)benzoyl)oxy)ethoxy)-3-(phenylsulfonyl)-1,2,5-oxadiazole 2-Oxide (12a) The title compound was obtained starting from **10** and **6a**. White waxy solid; yield: 62%. Analytical data for **12a**: IR (KBr, cm⁻¹): 3433, 2925, 1746, 1622, 1446, 1211, 1018; MS (ESI) m/z =476 [M+H]⁺; ¹H-NMR (DMSO-*d*₆, 300 MHz, δ ppm): 8.63 (br, 1H), 8.04 (d, 2H, J =7.8 Hz, Ar-H), 7.84 (d, J =7.8 Hz, 2H, Ar-H), 7.73 (m, 1H, Ar-H), 7.52–7.63 (m, 4H, Ar-H), 7.48 (d, J =16.2 Hz, 1H, CH=), 6.55 (d, J =16.2 Hz, 1H, CH=), 4.59 (t, 2H, J =4.8 Hz, OCH₂), 4.49 (t, 2H, J =4.8 Hz, OCH₂); ESI-HR-MS (m/z): [M+H]⁺ Calcd for C₂₀H₁₈N₃O₉S: 476.0764; Obsd: 476.0770; Anal. Calcd for C₂₀H₁₇N₃O₉S: C, 50.53; H, 3.60; N, 8.84; Found: C, 50.36; H, 3.69; N, 8.62.

(E)-4-(3-(((4-(3-(Hydroxyamino)-3-oxoprop-1-en-1-yl)benzoyl)oxy)propoxy)-3-(phenylsulfonyl)-1,2,5-oxadiazole 2-Oxide (12b) The title compound was obtained starting from **10** and **6b**. White waxy solid, yield: 65%. Analytical data for **12b**: IR (KBr, cm⁻¹): 3441, 2930, 1732, 1615, 1450, 1232, 1035; MS (ESI) m/z =490 [M+H]⁺; ¹H-NMR (DMSO-*d*₆, 300 MHz, δ ppm): 10.27 (br, 1H), 8.56 (br, 1H), 8.00 (d, 2H, J =7.8 Hz, Ar-H), 7.81 (d, J =7.8 Hz, 2H, Ar-H), 7.70 (m, 1H, Ar-H), 7.51–7.65 (m, 4H, Ar-H), 7.46 (d, J =16.2 Hz, 1H, CH=), 6.52 (d, J =16.2 Hz, 1H, CH=), 4.61 (t, 2H, J =4.8 Hz, OCH₂),

4.50 (t, 2H, $J=4.8$ Hz, OCH₂), 2.39 (m, 2H, OCH₂CH₂); ESI-HR-MS (m/z): [M+H]⁺ Calcd for C₂₁H₂₀N₃O₉S: 490.0920; Found: 490.0915; *Anal.* Calcd for C₂₁H₁₉N₃O₉S: C, 51.53; H, 3.91; N, 8.59; Found: C, 51.38; H, 4.02; N, 8.46.

(E)-4-(4-((4-(3-(Hydroxyamino)-3-oxoprop-1-en-1-yl)-benzoyl)oxy)butoxy)-3-(phenylsulfonyl)-1,2,5-oxadiazole 2-Oxide (12c) The title compound was obtained starting from **10** and **6c**. Pale yellow waxy solid, yield: 56%. Analytical data for **12c**: IR (KBr, cm⁻¹): 3452, 2965, 1716, 1611, 1444, 1242, 1168, 1052; MS (ESI) $m/z=504$ [M+H]⁺; ¹H-NMR (DMSO-*d*₆, 300MHz, δ ppm): 8.47 (br, 1H), 8.02 (d, 2H, $J=7.8$ Hz, Ar-H), 7.79 (d, $J=7.8$ Hz, 2H, Ar-H), 7.71 (m, 1H, Ar-H), 7.53–7.66 (m, 4H, Ar-H), 7.44 (d, $J=16.2$ Hz, 1H, CH=), 6.51 (d, $J=16.2$ Hz, 1H, CH=), 4.63 (t, 2H, $J=4.8$ Hz, OCH₂), 4.53 (t, 2H, $J=4.8$ Hz, OCH₂), 2.26–2.33 (m, 2H, OCH₂CH₂CH₂); ESI-HR-MS (m/z): [M+H]⁺ Calcd for C₂₂H₂₂N₃O₉S: 504.1077; Found: 504.1084; *Anal.* Calcd for C₂₂H₂₁N₃O₉S: C, 52.48; H, 4.20; N, 8.35; Found: C, 52.33; H, 4.38; N, 8.17.

(E)-4-((4-((4-(3-(Hydroxyamino)-3-oxoprop-1-en-1-yl)-benzoyl)oxy)but-2-yn-1-yl)oxy)-3-(phenylsulfonyl)-1,2,5-oxadiazole 2-Oxide (12d) The title compound was obtained starting from **10** and **6d**. Pale yellow waxy solid, yield: 53%. Analytical data for **12d**: IR (KBr, cm⁻¹): 3420, 2931, 1710, 1615, 1450, 1170, 1020; MS (ESI) $m/z=500$ [M+H]⁺; ¹H-NMR (DMSO-*d*₆, 300MHz, δ ppm): 8.55 (br, 1H), 8.08 (d, 2H, $J=7.8$ Hz, Ar-H), 7.83 (d, $J=7.8$ Hz, 2H, Ar-H), 7.75 (m, 1H, Ar-H), 7.55–7.67 (m, 4H, Ar-H), 7.51 (d, $J=16.2$ Hz, 1H, CH=), 6.57 (d, $J=16.2$ Hz, 1H, CH=), 5.11 (s, 2H, OCH₂), 5.03 (s, 2H, OCH₂); ESI-HR-MS (m/z): [M+H]⁺ Calcd for C₂₂H₁₈N₃O₉S: 500.0764; Found: 500.0758; *Anal.* Calcd for C₂₂H₁₇N₃O₉S: C, 52.91; H, 3.43; N, 8.41; Found: C, 53.12; H, 3.37; N, 8.55.

(E)-4-((4-((4-(3-(Hydroxyamino)-3-oxoprop-1-en-1-yl)-benzoyl)oxy)butan-2-yl)oxy)-3-(phenylsulfonyl)-1,2,5-oxadiazole 2-Oxide (12e) The title compound was obtained starting from **10** and **6e**. Pale yellow waxy solid, yield: 61%. Analytical data for **12e**: IR (KBr, cm⁻¹): 3432, 2939, 1728, 1622, 1458, 1210, 1021; MS (ESI) $m/z=504$ [M+H]⁺; ¹H-NMR (DMSO-*d*₆, 300MHz, δ ppm): 10.28 (br, 1H), 8.49 (br, 1H), 8.06 (d, 2H, $J=7.8$ Hz, Ar-H), 7.88 (d, $J=7.8$ Hz, 2H, Ar-H), 7.76 (m, 1H, Ar-H), 7.56–7.68 (m, 4H, Ar-H), 7.50 (d, $J=16.2$ Hz, 1H, CH=), 6.56 (d, $J=16.2$ Hz, 1H, CH=), 4.56 (t, 2H, $J=4.8$ Hz, OCH₂), 4.35 (m, 2H, OCH), 2.25–2.30 (m, 2H, OCHCH₂), 1.45 (d, 3H, $J=6.3$ Hz, CHCH₃); *Anal.* Calcd for C₂₂H₂₂N₃O₉S: 504.1077; Found: 504.1072; *Anal.* Calcd for C₂₂H₂₁N₃O₉S: C, 52.48; H, 4.20; N, 8.35; Found: C, 52.61; H, 4.33; N, 8.27.

(E)-4-(2-(4-(3-(Hydroxyamino)-3-oxoprop-1-en-1-yl)-benzamido)ethoxy)-3-(phenylsulfonyl)-1,2,5-oxadiazole 2-Oxide (12f) The title compound was obtained starting from **10** and **6f**. Pale yellow waxy solid, yield: 61%. Analytical data for **12f**: IR (KBr, cm⁻¹): 3436, 2945, 1621, 1453, 1211, 1166, 1018; MS (ESI) $m/z=477$ [M+H]⁺; ¹H-NMR (DMSO-*d*₆, 300MHz, δ ppm): 10.21 (br, 1H), 8.65 (br, 1H), 8.04 (d, 2H, $J=7.8$ Hz, Ar-H), 7.85 (d, $J=7.8$ Hz, 2H, Ar-H), 7.70 (m, 1H, Ar-H), 7.63 (d, $J=7.8$ Hz, 2H, Ar-H), 7.55 (m, 2H, Ar-H), 7.49 (d, $J=16.2$ Hz, 1H, CH=), 6.55 (d, $J=16.2$ Hz, 1H, CH=), 4.60 (t, 2H, $J=4.8$ Hz, OCH₂), 3.92 (t, 2H, $J=4.8$ Hz, NCH₂); ESI-HR-MS (m/z): [M+H]⁺ Calcd for C₂₀H₁₉N₄O₈S: 475.0924; Found: 475.0919; *Anal.* Calcd for C₂₀H₁₈N₄O₈S: C, 50.63; H, 3.82; N, 11.81; Found: C, 50.45; H, 4.01; N, 11.64.

(E)-4-(3-(4-(3-(Hydroxyamino)-3-oxoprop-1-en-1-yl)-benzamido)propoxy)-3-(phenylsulfonyl)-1,2,5-oxadiazole 2-Oxide (12g) The title compound was obtained starting from **10** and **6g**. Pale yellow waxy solid, yield: 58%. Analytical data for **12g**: IR (KBr, cm⁻¹): 3425, 2946, 1718, 1617, 1431, 1234, 1165; MS (ESI) $m/z=489$ [M+H]⁺; ¹H-NMR (DMSO-*d*₆, 300MHz, δ ppm): 10.33 (br, 1H), 8.52 (br, 1H), 8.02 (d, 2H, $J=7.8$ Hz, Ar-H), 7.83 (d, $J=7.8$ Hz, 2H, Ar-H), 7.73 (m, 1H, Ar-H), 7.58–7.66 (m, 4H, Ar-H), 7.46 (d, $J=16.2$ Hz, 1H, CH=), 6.52 (d, $J=16.2$ Hz, 1H, CH=), 4.59 (t, 2H, $J=4.8$ Hz, OCH₂), 3.55 (t, 2H, $J=4.8$ Hz, NCH₂), 2.32 (m, 2H, OCH₂CH₂); ESI-HR-MS (m/z): [M+H]⁺ Calcd for C₂₁H₂₁N₄O₈S: 489.1080; Found: 489.1077; *Anal.* Calcd for C₂₁H₂₀N₄O₈S: C, 51.64; H, 4.13; N, 11.47; Found: C, 51.83; H, 3.98; N, 11.23.

(E)-4-(4-(4-(3-(Hydroxyamino)-3-oxoprop-1-en-1-yl)-benzamido)butoxy)-3-(phenylsulfonyl)-1,2,5-oxadiazole 2-Oxide (12h) The title compound was obtained starting from **10** and **6h**. Pale yellow waxy solid, yield: 52%. Analytical data for **12h**: IR (KBr, cm⁻¹): 3429, 2944, 1724, 1620, 1441, 1220, 1032; MS (ESI) $m/z=503$ [M+H]⁺; ¹H-NMR (DMSO-*d*₆, 300MHz, δ ppm): 10.26 (br, 1H), 8.48 (br, 1H), 8.06 (d, 2H, $J=7.8$ Hz, Ar-H), 7.87 (d, $J=7.8$ Hz, 2H, Ar-H), 7.77 (m, 1H, Ar-H), 7.56–7.64 (m, 4H, Ar-H), 7.48 (d, $J=16.2$ Hz, 1H, CH=), 6.56 (d, $J=16.2$ Hz, 1H, CH=), 4.60 (t, 2H, $J=4.8$ Hz, OCH₂), 3.57 (t, 2H, $J=4.8$ Hz, NCH₂), 2.06–2.11 (m, 2H, OCH₂CH₂CH₂); ESI-HR-MS (m/z): [M+H]⁺ Calcd for C₂₂H₂₃N₄O₈S: 503.1237; Found: 503.1241; *Anal.* Calcd for C₂₂H₂₂N₄O₈S: C, 52.58; H, 4.41; N, 11.15; Found: C, 52.43; H, 6.59; N, 11.06.

(E)-4-((1-(4-(3-(Hydroxyamino)-3-oxoprop-1-en-1-yl)-benzamido)propan-2-yl)oxy)-3-(phenylsulfonyl)-1,2,5-oxadiazole 2-Oxide (12i) The title compound was obtained starting from **10** and **6i**. Pale yellow waxy solid, yield: 55%. Analytical data for **12i**: IR (KBr, cm⁻¹): 3414, 2928, 1717, 1615, 1425, 1235, 1052; MS (ESI) $m/z=489$ [M+H]⁺; ¹H-NMR (DMSO-*d*₆, 300MHz, δ ppm): 10.31 (br, 1H), 8.45 (br, 1H), 8.03 (d, 2H, $J=7.8$ Hz, Ar-H), 7.81 (d, $J=7.8$ Hz, 2H, Ar-H), 7.75 (m, 1H, Ar-H), 7.54–7.63 (m, 4H, Ar-H), 7.48 (d, $J=16.2$ Hz, 1H, CH=), 6.54 (d, $J=16.2$ Hz, 1H, CH=), 4.53 (m, 1H, OCH), 3.88 (m, 2H, NCH₂), 1.48 (d, 3H, $J=6.3$ Hz, CHCH₃); ESI-HR-MS (m/z): [M+H]⁺ Calcd for C₂₁H₂₁N₄O₈S: 489.1080; Found: 489.1086; *Anal.* Calcd for C₂₁H₂₀N₄O₈S: C, 51.64; H, 4.13; N, 11.47; Found: C, 51.39; H, 4.31; N, 11.62.

(E)-4-(2-(4-(3-(Hydroxyamino)-3-oxoprop-1-en-1-yl)-*N*-methylbenzamido)ethoxy)-3-(phenylsulfonyl)-1,2,5-oxadiazole 2-Oxide (12j) The title compound was obtained starting from **10** and **6j**. Pale yellow waxy solid, yield: 60%. Analytical data for **12j**: IR (KBr, cm⁻¹): 3426, 2935, 1719, 1626, 1440, 1243, 1162; MS (ESI) $m/z=489$ [M+H]⁺; ¹H-NMR (DMSO-*d*₆, 300MHz, δ ppm): 10.23 (br, 1H), 8.38 (br, 1H), 8.07 (d, 2H, $J=7.8$ Hz, Ar-H), 7.87 (d, $J=7.8$ Hz, 2H, Ar-H), 7.78 (m, 1H, Ar-H), 7.57–7.66 (m, 4H, Ar-H), 7.50 (d, $J=16.2$ Hz, 1H, CH=), 6.57 (d, $J=16.2$ Hz, 1H, CH=), 4.68 (t, 2H, $J=4.8$ Hz, OCH₂), 3.53 (t, 2H, $J=4.8$ Hz, NCH₂), 3.04 (s, 3H, NCH₃); ESI-HR-MS (m/z): [M+H]⁺ Calcd for C₂₁H₂₁N₄O₈S: 489.1080; Found: 489.1075; *Anal.* Calcd for C₂₁H₂₀N₄O₈S: C, 51.64; H, 4.13; N, 11.47; Found: C, 51.77; H, 4.22; N, 11.58.

Cell Culture SW620, HCT116, Lovo (human colon carcinoma cells), MCF-7 (human breast adenocarcinoma cells), and Hela cells were maintained in 10% fetal bovine serum

Dulbecco's modified Eagle's medium (FBS DMEM) medium (Gibco, Invitrogen), which were supplemented with 10% fetal calf serum (PAA, Austria) and antibiotics [100IU/mL penicillin and 100IU/mL streptomycin (Amresco)]. All of the cell lines were purchased from the Shanghai Institute of Cell Biology (Shanghai, China) and were grown at 37°C in a 5% CO₂ atmosphere.

MTT Assay The inhibitory effects on cell proliferation of test compounds were investigated by the MTT method. SW620, HCT116, Lovo, MCF-7, and Hela cells at a final density of 1.0×10^4 cells/well were placed in 96-well cell plates overnight and treated with or without different concentrations of test compounds for various periods of time. During the last 4h culture, the cells were exposed to MTT (5mg/mL), and the resulting formazan crystals were dissolved in 150 μ L of DMSO and measured using a spectrophotometer (Tecan) at a test wavelength of 570nm. Experiments were conducted in triplicate. Inhibition rate (%) = $[(A_{\text{control}} - A_{\text{treated}}) / A_{\text{control}}] \times 100\%$.

In Vitro HDACs Inhibition Fluorescence Assay *In vitro* HDACs inhibition assays were conducted according to the literature.³¹⁾ In brief, 10 μ L of enzyme solution (HeLa nuclear extract, HDAC2, HDAC6, or HDAC8) was mixed with various concentrations of tested compound. Five minutes later, fluorogenic substrate Boc-Lys (acetyl)-AMC (40 μ L) was added, and the mixture was incubated at 37°C for 30min and then stopped by addition of 100 μ L of developer containing trypsin and TSA. After incubation at 37°C for 20min, fluorescence intensity was measured using a microplate reader at excitation and emission wavelengths of 390 and 460nm, respectively. The inhibition ratios were calculated from the fluorescence intensity readings of tested wells relative to those of control wells, and the IC₅₀ values were calculated using a regression analysis of the concentration/inhibition data.

Nitrate/Nitrite Measurement in Vitro The levels of nitrate/nitrite produced by individual compounds in the cells were determined by the colorimetric assay using the nitrate/nitrite colorimetric assay kit (Beyotime, China), according to the manufacturer's instructions. Briefly, HCT116 cells (1×10^6 /well) were treated with the indicated concentrations of test compounds, and the nitrate/nitrite contents of the cell lysates were detected by the Griess assay. The absorbance was read at 540nm on a spectrophotometer (Smart spec, Bio-Rad). The cells treated with diluent were used as negative controls for the background levels of nitrate/nitrite production, while with sodium nitrate at different concentrations was used as positive controls for the standard curve.

References

- 1) Kelly T. K., de Carvalho D. D., Jones P. A., *Nat. Biotechnol.*, **28**, 1069–1078 (2010).
- 2) Blair L. P., Yan Q., *DNA Cell Biol.*, **31** (Suppl. 1), S49–S61 (2012).
- 3) Bolden J. E., Peart M. J., Johnstone R. W., *Nat. Rev. Drug Discov.*, **5**, 769–784 (2006).
- 4) Witt O., Deubzer H. E., Milde T., Oehme I., *Cancer Lett.*, **277**, 8–21 (2009).
- 5) Minucci S., Pelicci P. G., *Nat. Rev. Cancer*, **6**, 38–51 (2006).
- 6) Bertrand P., *Eur. J. Med. Chem.*, **45**, 2095–2116 (2010).
- 7) Paris M., Porcelloni M., Binaschi M., Fattori D., *J. Med. Chem.*, **51**, 1505–1529 (2008).
- 8) Glozak M. A., Seto E., *Oncogene*, **26**, 5420–5432 (2007).
- 9) Marks P. A., *Expert Opin. Investig. Drugs*, **19**, 1049–1066 (2010).
- 10) "FDA approval and new drug application (NDA) documents for Zolinza (SAHA, vorinostat)": http://www.accessdata.fda.gov/drugsatfda_docs/nda/2006/021991s000_ZolinzaTOC.cfm.
- 11) Coiffier B., Pro B., Prince H. M., Foss F., Sokol L., Greenwood M., Caballero D., Morschhauser F., Wilhelm M., Pinter-Brown L., Padmanabhan Iyer S., Shustov A., Nielsen T., Nichols J., Wolfson J., Balser B., Horwitz S., *J. Hematol. Oncol.*, **7**, 11 (2014).
- 12) McDermott J., Jimeno A., *Drugs Today (Barc.)*, **50**, 337–345 (2014).
- 13) Atadja P., *Cancer Lett.*, **280**, 233–241 (2009).
- 14) Zorzi A. P., Bernstein M., Samson Y., Wall D. A., Desai S., Nicksy D., Wainman N., Eisenhauer E., Baruchel S., *Pediatr. Blood Cancer*, **60**, 1868–1874 (2013).
- 15) Rao-Bindal K., Koshkina N. V., Stewart J., Kleinerman E. S., *Curr. Cancer Drug Targets*, **13**, 411–422 (2013).
- 16) Bumber Y., Younes A., Garcia-Manero G., *Expert Opin. Investig. Drugs*, **20**, 823–829 (2011).
- 17) Kang H., Gillespie T. W., Goodman M., Brodie S. A., Brandes M., Ribeiro M., Ramalingam S. S., Shin D. M., Khuri F. R., Brandes J. C., *Cancer*, **120**, 1394–1400 (2014).
- 18) Santo L., Hideshima T., Kung A. L., Tseng J. C., Tamang D., Yang M., Jarpe M., van Duzer J. H., Mazitschek R., Ogier W. C., Cirstea D., Rodig S., Eda H., Scullen T., Canavese M., Bradner J., Anderson K. C., Jones S. S., Raje N., *Blood*, **119**, 2579–2589 (2012).
- 19) Miller T. A., Witter D. J., Belvedere S., *J. Med. Chem.*, **46**, 5097–5116 (2003).
- 20) Paris M., Porcelloni M., Binaschi M., Fattori D., *J. Med. Chem.*, **51**, 1505–1529 (2008).
- 21) Fukumura D., Kashiwagi S., Jain R. K., *Nat. Rev. Cancer*, **6**, 521–534 (2006).
- 22) Bonavida B., Baritaki S., Huerta-Yepez S., Vega M. I., Chatterjee D., Yeung K., *Nitric Oxide*, **19**, 152–157 (2008).
- 23) Maksimovic-Ivanic D., Mijatovic S., Harhaji L., Miljkovic D., Dabideen D., Fan Cheng K., Mangano K., Malaponte G., Al-Abed Y., Libra M., Garotta G., Nicoletti F., Stosic-Grujicic S., *Mol. Cancer Ther.*, **7**, 510–520 (2008).
- 24) Huang Z., Zhang Y., Zhao L., Jing Y., Lai Y., Zhang L., Guo Q., Yuan S., Zhang J., Chen L., Peng S., Tian J., *Org. Biomol. Chem.*, **8**, 632–639 (2010).
- 25) Ling Y., Ye X., Ji H., Zhang Y., Lai Y., Peng S., Tian J., *Bioorg. Med. Chem.*, **18**, 3448–3456 (2010).
- 26) Ling Y., Ye X., Zhang Z., Zhang Y., Lai Y., Ji H., Peng S., Tian J., *J. Med. Chem.*, **54**, 3251–3259 (2011).
- 27) Han C., Huang Z., Zheng C., Wan L., Zhang L., Peng S., Ding K., Ji H., Tian J., Zhang Y., *J. Med. Chem.*, **56**, 4738–4748 (2013).
- 28) Illi B., Colussi C., Grasselli A., Farsetti A., Capogrossi M. C., Gaetano C., *Pharmacol. Ther.*, **123**, 344–352 (2009).
- 29) Borretto E., Lazzarato L., Spallotta F., Cencioni C., D'Alessandra Y., Gaetano C., Fruttero R., Gasco A. *ACS Med. Chem. Lett.*, **4**, 994–999 (2013).
- 30) Colussi C., Mozzetta C., Gurtner A., Illi B., Rosati J., Straino S., Ragone G., Pescatori M., Zaccagnini G., Antonini A., Minetti G., Martelli F., Piaggio G., Gallinari P., Steinkuhler C., Clementi E., Dell'Aversana C., Altucci L., Mai A., Capogrossi M. C., Puri P. L., Gaetano C., *Proc. Natl. Acad. Sci. U.S.A.*, **105**, 19183–19187 (2008).
- 31) Prince H. M., Bishton M. J., Harrison S. J., *Clin. Cancer Res.*, **15**, 3958–3969 (2009).